Journal of Alloys and Compounds 509 (2011) 6626–6630

Contents lists available at ScienceDirect

Journal of Alloys and Compounds

journal homepage: www.elsevier.com/locate/jallcom

Enhanced exchange bias of isolated Co/CoO nanocaps

Y.X. Wang, N.N. Yang, M.B. Wei, Y.J. Zhang, H.B. LiuY. Liu, J.H. Yang*

Institute of Solid State Physics of Jilin Normal University, Jilin 136000, PR China

ARTICLE INFO

Article history:
Received 10 November 2010
Received in revised form 17 March 2011
Accepted 18 March 2011
Available online 29 March 2011

PACS:
75.30.Et
75.70.Cn

Keywords:
Exchange-bias(EB)
Nanocaps
Co/CoO bilayer
Curved substrate

ABSTRACT

We demonstrated the fabrication of the isolated magnetic Co/CoO nanocap array by oxidating the single Co layer which was deposited onto the two dimensional polystyrene sphere array. Compared to the continuous film and thicker nanocap structure, H_E and H_C of the 15 nm Co/CoO isolated cap array were enhanced significantly and were about 4 times as those of the corresponding continuous film, which was ascribed to the formation of the isolated magnetic single domain state due to the magnetic limit around the cap brim after the oxidation treatment. When the beads of the different sizes were used as the substrate, H_E increased when the bead size decreased, which was ascribed to the increase of the localized uncompensated CoO spins.

1. Introduction

The exchange bias phenomenon of the bilayer composed of ferromagnetic (F) and antiferromagnetic (AF) materials was extensively reported in many Refs. [1–3]. Its main characteristic was the shift of hysteresis loop along the field axis after the field cooling from above the blocking temperature T_B of the system. The physical origin of the exchange bias was generally accepted to be the exchange coupling between F and AF components at the interface. The coupled bilayers had the important applications in the hard drive and the magnetic random access memory (MRAM) [4,5]. In recent years, the exchange bias effects for the different nanostructure arrays, such as nanodot, nanoring, and nanowire, were studied widely in theory and experiment due to the increasing demand for the high density data storage [6–9]. For the nanostructure arrays, the size and shape became the very important factors to decide the magnetic properties, which were believed to originate from the structural modifications of the interfaces. Although there were many reports on the exchange bias of the nanostructures, most were based on the flat substrate and a small number of studies were on the curved substrate. To understand the exchange bias phenomenon of the curvature morphology, some reports studied the properties of the nanocap based on the spherical substrate [10–14]. The results showed that the curvatured morphology played an important action in the modification of the magnetic properties, but the magnetic interaction is inevitable between the neighbor spheres. However, for the patterned nanostructure array, the magnetic interactions between the units were a disadvantaged factor for the high density magnetic recording. Therefore, it is very important to fabricate the undamaged and isolated unite by the simple process. In this work we fabricated Co/CoO bilayer on the curved surfaces by oxidating the single layer Co. The exchange-isolated bilayer magnetic cap was formed by this method, and the direct magnetic contact between the neighbor magnetic units was reduced greatly. The magnetic properties of the isolated Co/CoO caps were investigated and the influence of the colloidal size on the exchange bias was analyzed.

2. Experimental

The densely packed two-dimensional arrays of monodisperse polystyrene colloid sphere (PS) with different sizes were prepared by the self-assembly technique on the Si wafer (Fig. 1). The ordered spherical surfaces were used as the curved substrate for the film deposition. The detailed fabrication method was given in our previous work [15]. The colloidal polystyrene solution (10 wt.% in water) was purchased from the Duke scientific corporation. The monolayer Co with the different thickness was deposited onto the PS arrays in magnetron sputtering system by dc sputtering the Co materials. The base pressure was 2×10^{-6} Pa and the argon pressure was 0.4 Pa during film deposition. For comparison, the single Co film was grown directly on the Si wafer with the same experimental setting. All the samples were oxidized at 373 K for 5 h under oxygen atmosphere. The elements of the film were characterized by PHI 550 multifunctional X-ray photoelectron spectroscopy (XPS). The scanning electron microscopy (SEM) images were recorded on a JEOL 6500F, a

* Corresponding author. Tel.: +86 434 3294566.
E-mail address: jhyang1@jlnu.edu.cn (J.H. Yang).

0925-8388/$ – see front matter © 2011 Elsevier B.V. All rights reserved.
doi:10.1016/j.jallcom.2011.03.113

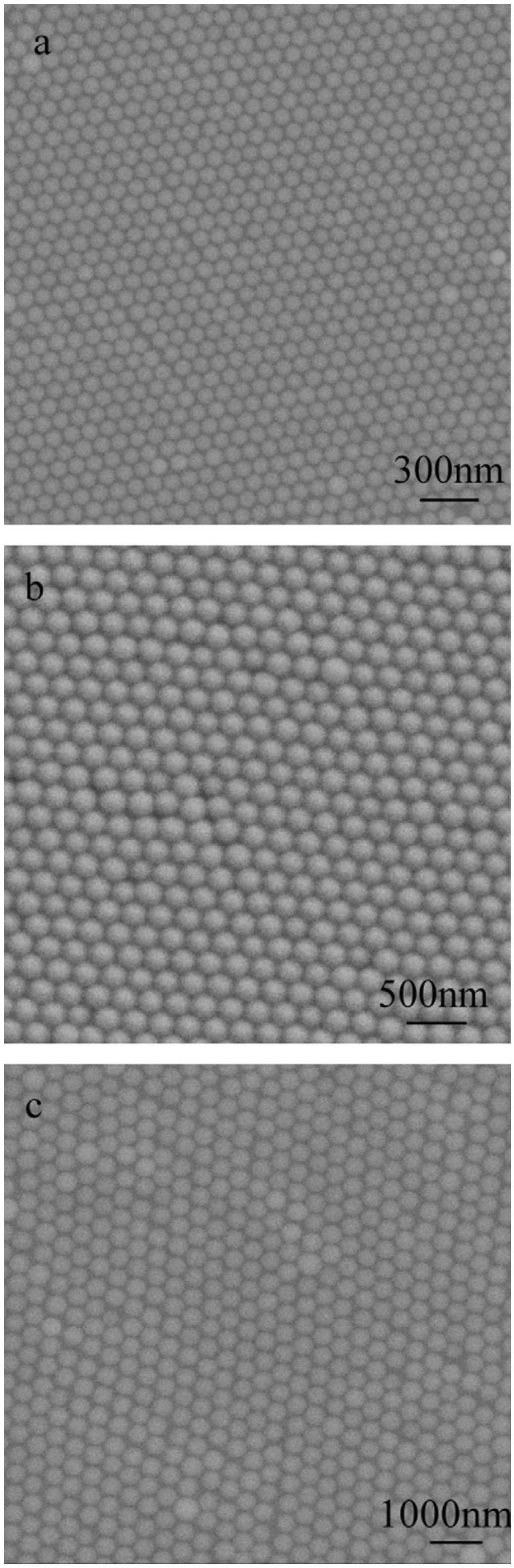

Fig. 1. SEM images for the monodisperse polystyrene colloid sphere arrays of the different diameter (a) 100 nm, (b) 200 nm and (c) 460 nm.

high resolution (1.5 nm) thermal field emission electron microscope, operating at 5.0 KV. Transmission electron microscopy (TEM) was performed on JEM-2100HR, operating at 200 keV. MFM was performed on a nanoscope III of Digital Instrument, and the lifted distance was 100 nm for the second scan. The samples were cooled in a magnetic field of 8 kOe from room temperature down to 90 K, and the magnetic hysteresis loops of the films were measured with a vibrating sample magnetometer (VSM) and a superconducting quantum interference devices magnetometer (SQUID, Quantum Design, MPMSXL-5).

3. Results and discussions

The surfaces of Co layer for all samples were oxidized when treated under oxygen atmosphere. Fig. 2 gave the XPS spectra of the oxidized 30 nm-Co on the PS. The peaks of Co $2p_{3/2}$ at 780.4 eV and Co $2p_{1/2}$ at 795.4 eV indicated the Co^{2+} existence at the surface of Co layer, which confirmed the formation of CoO on the sample surface. There were not signals from Co^{3+} ions detected by XPS. Even if there were a trace of Co^{3+} ions in the samples, they did not show the exchange bias effect when the measure temperature is 90 K, because the Néel temperature of AF material Co_3O_4 is only 40 K [16]. Fig. 3 showed the hysteresis loops of the Co/CoO bilayer with the different thickness on the 200 nm PS sphere array. The exchange bias field (H_E) of the film on the curved substrate was larger than that of the corresponding continuous film. And H_E increased when Co thickness decreased for both nanostructure and continuous bilayer due to the interface effect [17]. In addition, the differences between the nanostructures and continuous film became more and more prominent when Co thickness decreased. A step was observed in the hysteresis loop for Co 15 nm and Co 25 nm samples on the curved substrate respectively, and the hysteresis loop for Co 30 nm sample did not show the step. When Co 30 nm was measured at 30 K by SQUIT, the sample did not show the step except for the increases of H_C and H_E. We believed that this phenomenon was related to the substrate topographic feature. When the Co film was deposited on the PS array, the caps array on the sphere surface and the dots array between the spheres formed simultaneously [10]. The combination of the signals from the caps and the dots resulted in the step for the Co 15 nm and Co 25 nm film. For the Co 30 nm sample, the difference between two magnetic signals may be so small that the step was not obvious, and the similar result was also reported in the previous researches [18].

For the Co 15 nm bilayer, H_E and H_C of the caps structure were almost as 4 times large as those of the corresponding continuous film. To decide origin of the large bias effect, from the magnetic cap on PS colloids or from the nanodots between the neighbor beads, we removed the magnetic caps by etching the colloids and the magnetic dots were left on the Si substrate. The hysteresis loop of the dots array was shown in Fig. 4, and the inset was the SEM image of the nanodot. The magnetic observations showed H_E of the nanodots was around zero. However, HRTEM result showed the surfaces of the dots were oxidized due to the heating treatment in oxygen. For 200 nm colloid template, the lateral size of a dot is about 46 nm

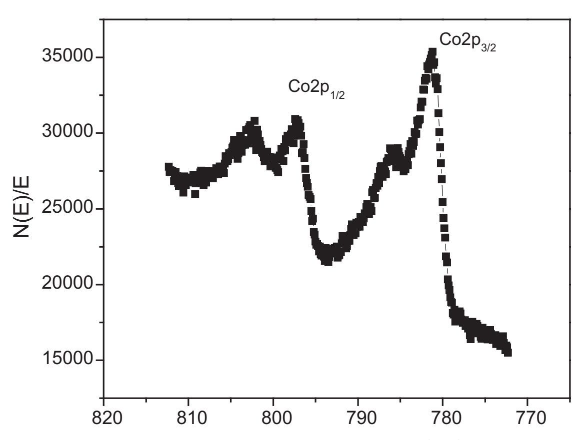

Fig. 2. X-ray photoelectron spectroscopy for Co films after oxidation.

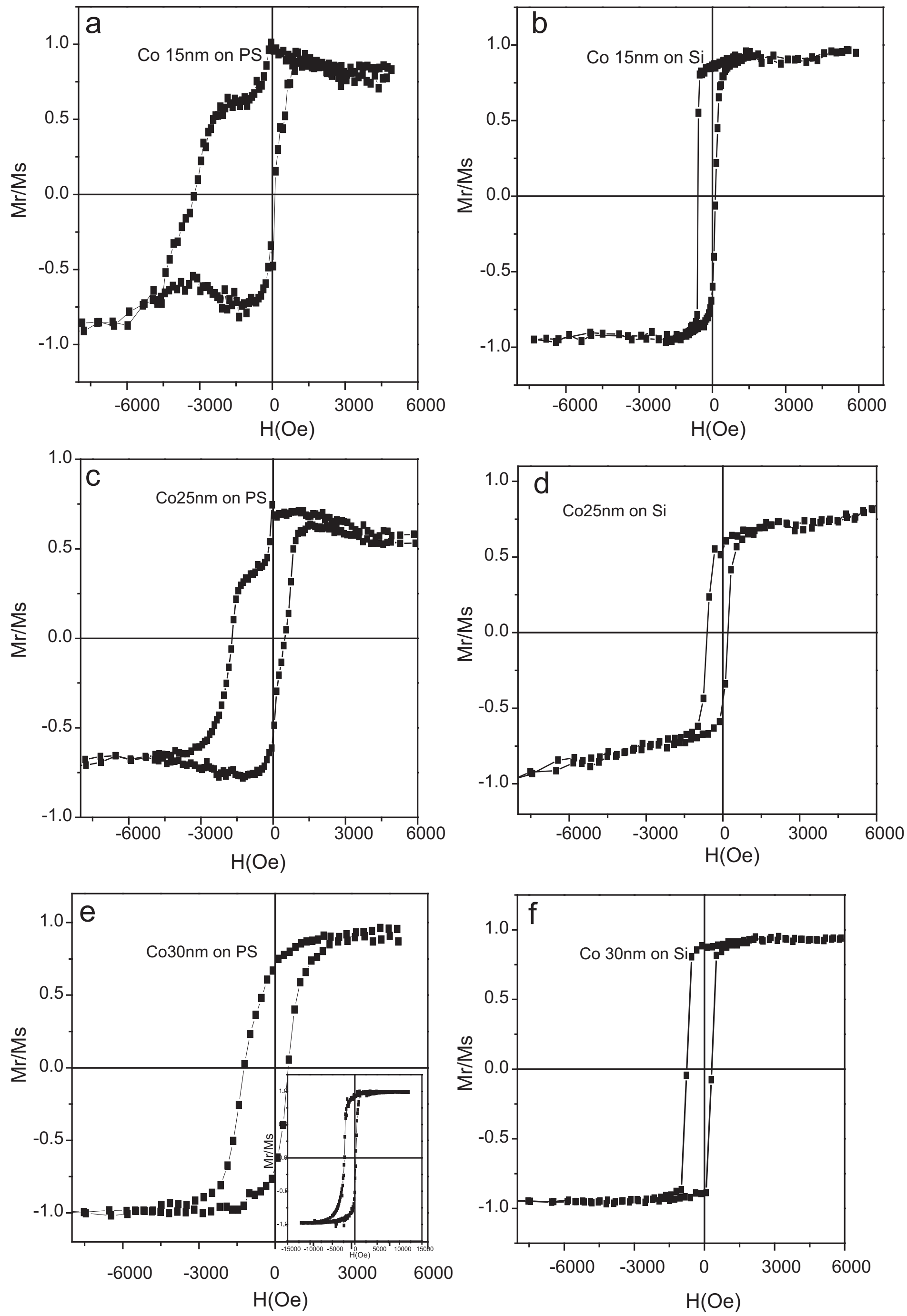

Fig. 3. Hysteresis loops for the Co/CoO bilayer with the different Co thickness on 200 nm colloidal beads (a and b) Co 15 nm; (c and d) Co 25 nm; (e and f) Co 30 nm and corresponding Si substrate. The hysteresis loop of the set was measured by SQUIT at 30 K and the substrate signal was deducted.

and the separation was 115 nm between the neighbor nanodots [19]. And the height decreased about 30% compared to the nominal thickness due to the shadowing effect induced by the colloid sphere [20]. We believed that the AF CoO layer showed the reduced pinning effect at 90 K due to the lower thermal stability for the very small pattern system, and H_E is near zero [21]. These results indicated the large bias field and the coercivity were from the cap structure. TEM image showed the thickness of the magnetic cap decreased along the sphere surface (Fig. 5a). The HRTEM image showed the formation of the oxidized sublayer and the thickness of oxidized sublayer was about 2 nm (Fig. 5b). The bilayer structure was transformed into the single CoO layer around the cap brim, separating the magnetic caps from the neighbor ones. So the magnetic interactions between the neighbor caps were reduced greatly, which meant the isolated magnetic caps formed on every PS bead. The size of isolated Co/CoO bilayer was about 160 nm on every sphere from the TEM image, as shown by the line in Fig. 5c. The MFM image showed that the beads had the magnetic properties partially and were separated magnetically from the neighbor units, confirming the analysis above (Fig. 5d). A single-domain state formed in the 15 nm Co/CoO isolated magnetic cap. For a single-domain nanostructure, the value of the coercivity was estimated using $H_C \sim 2K_u/M$, where $K_u \sim DM^2/2$, and D was a dimensional constant which equaled the ratio of thickness (t) to the size (L) of the nanostructure [22]. The coercivity and the size satisfied $H_C \sim tM/L$. For our experiments, the parameters were as $t \sim 15$ nm, $L \sim 160$ nm, and $M \sim 1.7 \times 10^4$ Oe for

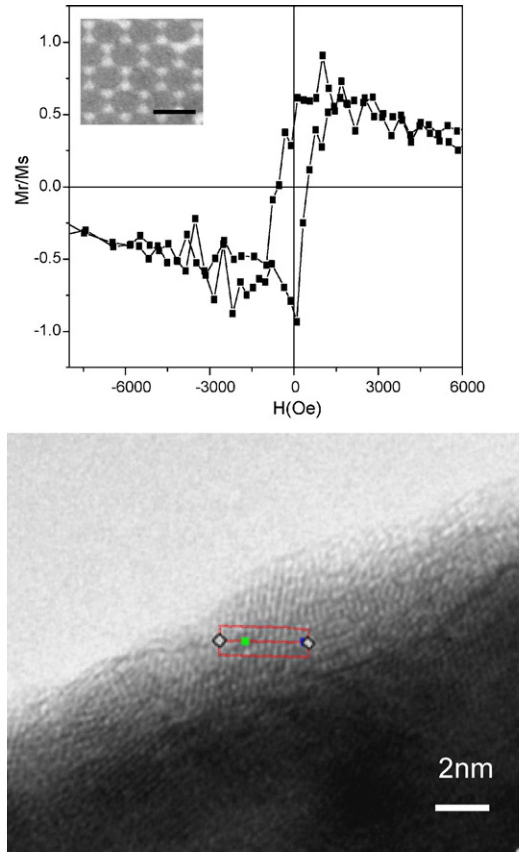

Fig. 4. Hysterisis loop of the dot left on Si substrate when the cap was removed for the Co 15 nm sample. The inset was the corresponding SEM image of the dot on the substrate and the scale bar was 300 nm. HRTEM showed the dot surface was oxidized and the *d* value was around 0.248 nm confirming the existence of CoO after the oxygen treatment.

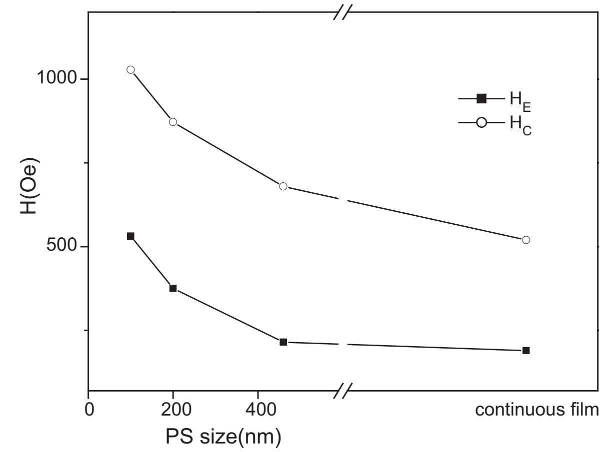

Fig. 6. Dependences of the coercivity and the bias field on the bead sizes for the oxidized Co 30 nm sample.

Co film. We calculated that the value of H_C was about 1600 Oe, in agreement with our experimental results. When the film thickness increased to 25 nm and 30 nm, the connection between the neighbor magnetic caps happened, which changed the isolated state and made H_E and H_C decrease.

In order to further understand the magnetic behavior of the curved interface, the PS particles with the different sizes were used for the Co film deposition with the same thickness. Fig. 6 showed the changes of H_C and H_E of the oxidized samples deposited on the flat and curved substrates. H_E and H_C for the latter were larger than the former and they increased when the bead size decreased. For the curved bilayer with the same thickness, the change of H_E was mainly from the variation of colloid sphere sizes. It was known that the exchange bias was related to the density of the uncompensated AF material interfacial spin, especially for CoO material with the high magnetocrystalline anisotropy [23]. The smaller beads meant

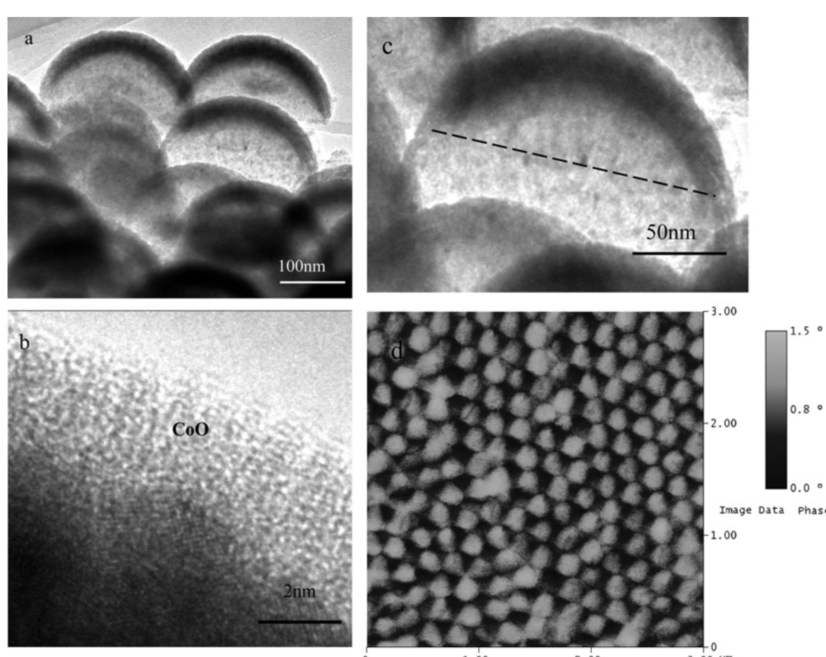

Fig. 5. TEM and HRTEM images showed the formation of the Co/CoO bilayer cap by the oxidation treatment on 200 nm colloid sphere (a and b). And only part of the magnetic cap showed the exchange coupling effect (c and d).

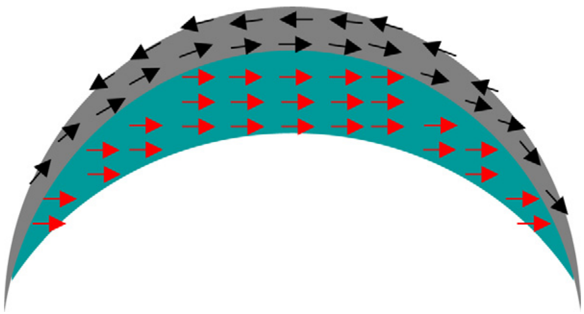

Fig. 7. Sketch map of the localized uncompensated interfacial spins for the curved film.

the larger curvature and the larger interfacial roughness. To relieve the stress the crystalline orientation of CoO became more complicated and the grain boundaries increased correspondingly [24]. These structural defects created more localized uncompensated interfacial spins around the cap brim as shown in the sketch map of spin structure (Fig. 7). The uncompensated spins exerted a strong torque on these Co spins by coupling to them, which enhanced the exchange bias field. The surface anisotropy and defects in the curved interfaces created the large localized field and enhanced the static magnetic interaction, which led to the increase of the coercivity [25].

4. Conclusions

In conclusion, the Co/CoO curved bilayers were fabricated by oxidating the single layer Co deposited on the colloidal sphere array. When Co thickness decreased, H_E increased and the difference of H_E became more prominent between curved film and corresponding flat film. The enhancements of H_E and H_C for Co 15 nm cap array were ascribed to the formation of the isolated magnetic single domain state due to the magnetic limit around the cap brim after the oxidation treatment. H_E increased with the decrease of the colloid sphere sizes. And H_E and H_C of the curved film were larger than those of the continuous films, which were ascribed to the increase of the localized uncompensated CoO spins induced by the curved surface.

Acknowledgements

This work is supported partly by National Programs for High Technology Research and Development of China (No. 2009AA03Z303), the National Youth Program Foundation of China (No. 10804036 and 10904050), and Program for New Century Excellent Talents in University (No. NCET-09-0156), Program for the development of Science and Technology of Jilin province (No. 20100547, 20090331, 20090531 and 20082112).

References

[1] W.H. Meiklejohn, C.P. Bean, Phys. Rev. 105 (1957) 904.
[2] P. Miltényi, M. Gierlings, J. Keller, B. Beschoten, G. Güntherodt, U. Nowak, K.D. Usadel, Phys. Rev. Lett. 84 (2000) 4224.
[3] B. Beckmann, U. Nowak, K.D. Usadel, Phys. Rev. Lett. 91 (2003) 187201.
[4] V. Skumryev, S. Stoyanov, Y. Zhang, G. Hadjipanayis, D. Givord, J. Nogués, Nature 423 (2003) 850.
[5] J. Eisenmenger, I.K. Schuller, Nat. Mater. 2 (2003) 437.
[6] S. Tacchi, M. Madami, G. Gubbiotti, G. Carlotti, W. Jung, C.A. Ross, J. Appl. Phys. 103 (2008) 07C103.
[7] R.D. McMichael, V.P. Chuang, C.A. Ross, J. Appl. Phys. 103 (2008) 07C505.
[8] V. Salgueiriño-Maceira, M.A. Correa-Duarte, M. Bañobre-López, M. Grzelczak, M. Farle, L.M. Liz-Marzán, J. Rivas, Adv. Funct. Mater 18 (2008) 616.
[9] S.H. Chung, A. Hoffmann, M. Grimsditch, Phys. Rev. B 71 (2005) 214430.
[10] M. Albrecht, G. Hu, I.L. Guhr, T.C. Ulbrich, J. Boneberg, et al., Nat. Mater. 4 (2005) 203.
[11] C.M. Günther, O. Hellwig, A. Menzel, B. Pfau, F. Radu, D. Makarov, M. Albrecht, A. Goncharov, T. Schrefl, W.F. Schlotter, R. Rick, J. Lüning, S. Eisebitt, Phys. Rev. B 81 (2010) 064411.
[12] T.C. Ulbrich, D. Makarov, G. Hu, I.L. Guhr, D. Suess, T. Schre, M. Albrecht, Phys. Rev. Lett. 96 (2006) 077202.
[13] T. Eimüller, T.C. Ulbrich, E. Amaladass, I.L. Guhr, T. Tyliszczak, M. Albrecht, Phys. Rev. B 77 (2008) 134415.
[14] E. Amaladass, B. Ludescher, G. Sch1tz, T. Tyliszczak, M.S. Lee, T. Eimü1ler, J. Appl. Phys. 107 (2010) 053911.
[15] Y.J. Zhang, W. Li, K.J. Chen, J. Alloys Compd. 450 (2008) 512.
[16] S. Gangopadhyay, G.C. Hadjipanayis, C.M. Sorensen, J. Klabunde, J. Appl. Phys. 73 (1993) 6964.
[17] J. Nogués, I.K. Schuller, J. Magn. Magn. Mater. 192 (1999) 203.
[18] V. Baltz, J. Sort, S. Landis, B. Rodmacq, B. Dieny, Phys. Rev. Lett. 94 (2005) 117201.
[19] J.C. Hulteen, R.P. Van Duyne, J. Vac. Sci. Technol 13 (1995) 1553.
[20] Y.J. Zhang, Y.X. Wang, X.D. Meng, J.H. Yang, J. Appl. Phys. 105 (2009) 083910.
[21] V. Baltz, J. Sort, B. Rodmacq, B. Dieny, Phys. Rev. B 72 (2005) 104419.
[22] S.P. Li, W.S. Lew, Y.B. Xu, A. Hirohata, A. Samad, F. Baker, J.A.C. Bland, Appl. Phys. Lett. 76 (2000) 748.
[23] K. Takano, R.H. Kodama, A.E. Berkowitz, W. Cao, G. Thomas, Phys. Rev. Lett. 79 (1997) 1130.
[24] A.E. Berkowitz, K. Takano, J. Magn. Magn. Mater. 200 (1999) 552.
[25] D.H. Han, J.G. Zhu, J.H. Judy, J. Appl. Phys. 81 (1997) 4996.